

A Survey of Intrinsic Absorption in Active Galaxies using the Far Ultraviolet Spectroscopic Explorer¹

Jay P. Dunn², D. Michael Crenshaw², S. B. Kraemer³, & J. R. Gabel⁴

ABSTRACT

We present a survey of 72 Seyfert galaxies and quasars observed by the *Far Ultraviolet Spectroscopic Explorer (FUSE)*. We have determined that 72 of 253 available active galactic nuclei (AGN) targets are viable targets for detection of intrinsic absorption lines. We examined these spectra for signs of intrinsic absorption in the O VI doublet ($\lambda\lambda 1031.9, 1037.6$) and Lyman β ($\lambda 1025.7$). The fraction of Seyfert 1 galaxies and low-redshift quasars at $z \lesssim 0.15$ that show evidence of intrinsic UV absorption is $\sim 50\%$, which is slightly lower than Crenshaw et al. (1999) found (60%) based on a smaller sample of Seyfert 1 galaxies observed with the *Hubble Space Telescope (HST)*. With this new fraction we find a global covering factor of the absorbing gas with respect to the central nucleus of ~ 0.4 . Our survey is to date the largest searching for intrinsic UV absorption with high spectral resolution, and is the first step toward a more comprehensive study of intrinsic absorption in low-redshift AGN.

Subject headings: galaxies: Seyfert – ultraviolet: galaxies

1. Introduction

Seyfert galaxies are relatively nearby, mostly spiral galaxies that host active galactic nuclei (AGN). Intensive studies over the past few decades lead us to believe that a supermassive black hole with an accretion disk lies at the core of every active galaxy and is the engine

¹Based on observations made with the NASA-CNES-CSA Far Ultraviolet Spectroscopic Explorer. FUSE is operated for NASA by the Johns Hopkins University under NASA contract NAS5-32985.

²Department of Physics and Astronomy, Georgia State University, Atlanta, GA 30303. Email: dunn@chara.gsu.edu, crenshaw@chara.gsu.edu

³Institute for Astrophysics and Computational Sciences, Department of Physics, The Catholic University of America, Washington, DC 20064; kraemer@yancey.gsfc.nasa.gov.

⁴Physics Department, Creighton University, Omaha, NE 68138

driving the activity. Seyfert galaxies, unlike quasars, are typically close, with redshifts $z \lesssim 0.1$ and have moderate bolometric luminosities (10^{45} ergs s⁻¹). Over time scales ranging from days to years Seyfert galaxies show variation in continuum luminosity over a factor of ~ 10 in amplitude (Dunn et al. 2006). Seyfert galaxies are divided into two basic categories, 1 and 2 (Kachikian & Weedman 1974). Seyfert 1 galaxies show both broad permitted emission lines and narrow permitted and forbidden lines, while the UV and optical spectra of Seyfert 2 galaxies are devoid of broad emission features in unpolarized light.

Oke & Sargent in (1968) found that while the optical spectra of Seyferts have absorption features, which were previously attributed as stellar, there was an He I line in NGC 4151 that was likely due to self-absorption. Anderson & Kraft (1969) found 3 kinematic components within the He I and hydrogen Balmer absorption lines that showed blueshifts relative to the rest frame of up to 970 km s⁻¹. They attributed these features to an outflow of gas from the core with multiple kinematic components.

Cromwell & Weymann (1970) showed that the absorption was variable. Ulrich & Boisson (1983) found in data from the *International Ultraviolet Explorer (IUE)* that only 3 to 10% of Seyfert galaxies showed intrinsic absorption in high-ionization lines (C IV, N V, O VI). Crenshaw et al. (1999) found in an *HST* study that this number was far too low due to the low resolution of *IUE* and that the percentage of Seyfert galaxies that showed intrinsic C IV absorption was closer to 60%. This however was not a large survey, 17 objects, with possibly some selection biases. It did show that intrinsic absorption was much more prominent in Seyfert 1 galaxies than previously thought and that further study is required of this phenomenon to more fully understand the central engine in AGN. Crenshaw et al. also showed a 1:1 relationship between the warm X-Ray absorbers (George et al. 1998, Reynolds 1997) and intrinsic UV absorption in Seyfert galaxies. They also estimated a global covering factor for Seyfert galaxies of ~ 0.5 . Laor & Brandt (2002) surveyed 50 AGN that included both quasars and Seyfert galaxies. Their survey found that 44% showed C IV absorption with an equivalent width greater than 0.1 Å.

In a recent review article, Crenshaw, Kraemer, & George (2003) found that while there have been many advances in the field of intrinsic absorption, the need for further examination of mass outflow properties in AGN is necessary. We need to have a larger survey of AGN to investigate the effects of luminosity, AGN type, radio power, orientation and accretion rate. Also, there is a need to determine transverse velocities of the intrinsic absorbing clouds (as seen in Kraemer et al. 2001). These factors will help constrain dynamical models currently being considered as explanations of the origin of the mass outflow. This paper will be the first in a series designed to further our understanding of these characteristics. The main goal of the paper is to presents the spectra, component identifications, and the frequency of

occurrence of intrinsic absorption.

2. Survey

Our survey is more than 4 times larger than that of Crenshaw et al. 1999 and is taken from the available *FUSE* data at the *Multimission Archives at Space Telescope (MAST)* (url: <http://archive.stsci.edu/>). *FUSE* is ideal for intrinsic absorption studies in AGN due to the wavelength coverage (905 Å to 1187 Å) that allows for the O VI doublet ($\lambda\lambda 1031.9, 1037.6$) and Lyman β ($\lambda 1025.7$) to be detected at low redshifts. *FUSE* also lends itself to this work because of its resolution, approximately 15 km s^{-1} (FWHM), allowing us to find narrow absorption features and resolve structure in broader features.

FUSE is comprised of 4 mirrors and 4 gratings split on to two detectors (Sahnow 2002). This provides 8 different spectra per observation. One set uses a LiF coating while the other a SiC coating. The LiF coating provides a reflectivity nearly twice that of the SiC at wavelengths greater than 1050 Å. In nearly every spectrum, this implies a better signal-to-noise across the LiF spectrum in the region of interest. We downloaded the raw data for all of the targets we selected and processed them using CalFUSE v3.1 in time-tag mode (TTAG) (Dixon et al. 2002). We coadded 7 of the 8 spectra into one spectrum weighted by exposure time. We did not include the LiF 1b segment in the coadded spectrum. We intentionally omitted this because of a distortion (known as the "worm") in the spectrum for this segment that has no available correction. For objects with multiple epochs of observing we averaged the spectra. In a future paper, we will examine the absorption variability using the multi-epoch observations.

FUSE has no calibration lamp onboard, leaving wavelength calibration to ISM lines (Sahnow et al. 2000). This introduces a velocity error of approximately 20 km s^{-1} (Gillmon et al 2006), which is significant with a resolution of 15 km s^{-1} . However our survey's initial purpose is to find Seyfert galaxies that exhibit intrinsic absorption and provide approximate velocity centroids. In a subsequent paper, we will present measured velocities and velocity widths for all available absorption lines. Also, we will provide a good estimate of the velocity error for any given spectrum based on the position of various ISM lines seen in spectra on a target-by-target basis.

Our list of targets originated from the category listing on the *MAST* website. We took all targets listed by observers as Seyfert galaxies or as Quasars, 253 targets. Using the NASA Extragalactic Database (NED) (url: <http://nedwww.ipac.caltech.edu/index.html>), we narrowed the total list by eliminating any targets that had a redshift greater than $z \approx$

0.15, to 143 objects. Any target with a redshift greater than this places the O VI doublet outside of the wavelength coverage for *FUSE*. We have retained these data for possible further analysis of the C III line ($\lambda 977.03$) and the N III ($\lambda 989.79$) line.

We narrowed the list further to 122 objects, by removing any galaxy that had a type listed in NED other than Seyfert 1 or quasar; note that we still examined the spectra of these targets, but these were not included in the survey. We include only Seyfert 1 galaxies or quasars because detection of intrinsic absorption requires a strong background source (i.e. continuum and broad line region).

One interesting target that we removed is WPVS007. According to K. Leighly et al. (2007, in prep), this Seyfert galaxy has evolved to a Broad Absorption Line mini-quasar. Thus, we have eliminated it from our list, although it has been known to show narrow intrinsic absorption lines in previous observations (Crenshaw et al. 1999).

The last criterion that we applied to the data was a signal to noise cutoff. By utilizing the provided noise vector with the data we found a good cutoff for the signal-to-noise per resolution element ($\sim 15 \text{ km s}^{-1}$ FWHM) of 1.5 across the span 1050\AA to 1100\AA . Although this value appears to be low, there are many resolution elements across a typical intrinsic absorption line. In this region we have data from the LiF portion of the spectrograph as well as data from the SiC portion coadded to give a good overall estimate of the quality of the spectrum.

Table 1 lists our 72 AGN used in the survey. We list the signal-to-noise we found in this region for a coadded spectrum per object in Table 1. We also provide a list of the observations available per object in Table 1. In the case of NGC 3516 we did not use all available observations. We chose to use only the 2000 observation, ID P1110404, the LiF portion of the February 2006 observation and the January 2007 observation in our coadded spectrum. This set of spectra has a lower signal to noise, 1.9, than the total coadded spectrum, but these observations have no O I geocoronal dayglow interference, which is heavy in the O VI region of the spectrum.

3. Absorption Detection

3.1. Identification

In order to determine which lines are truly intrinsic versus lines that originate in our Galaxy's ISM, we used a program that provided a synthetic H_2 spectrum (Tumlinson et al. 2002), which we overlaid on our velocity plots. As an example, Figure 1 shows the

spectrum of IRAS F04250-5718. We have the blue member and red member of the O VI doublet and the Lyman β lines in respective order from top to bottom plotted in velocity space. The dashed line is the overlaid H₂ synthetic spectrum from the Tumlinson code, and the other lines are ISM lines, taken from Morton (1991), scaled to their oscillator strength. The program requires H₂ columns to be input for each rovibrational level of the molecule. For detection purposes we input exceptionally high values for the column for each rovibrational level (lower angular momentum level J=0 through 7), on the order of 10^{19} cm⁻². This was to remove any speculation as to whether a line was truly H₂ in origin or intrinsic to the AGN/host galaxy. For H₂ lines that were coincident with an possible intrinsic absorption feature, we examined nearby H₂ lines for both number and strength to place estimates on the contamination.

Another factor that presented problems was geocoronal dayglow emission lines. These are background lines from the Earth’s atmosphere that appear as narrow emission lines, which can have peak flux levels several times that of the surrounding continuum spectrum (Feldman et al. 2001). These lines are strong when *FUSE* is observing during the orbit day at low-Earth approach. One example is seen in NGC 4151 as Lyman β and O I dayglow near 1025 Å in Figure 2.

We visually examined the spectra for lines that did not match the H₂ synthetic spectra or the ISM lines. These were flagged for further examination. We identified clean absorption features that had components at approximately the same velocity in at least 2 of the available lines (the 2 members of the O VI doublet and Lyman β). Any absorption line that aligned in velocity space for 2 of the 3 available lines with at least 2σ in equivalent width was identified as intrinsic absorption. We recorded their approximate velocities based on plots similar to Figure 1, which we provide in Table 2. An example is IRAS F04250-5718. We can see in Figure 1 for IRAS F04250-5718 that intrinsic absorption appears in all three at relatively the same velocity with one broad component ranging between -300 and -100 km s⁻¹ and an additional component at approximately -100 km s⁻¹.

A handful of targets are still enigmas. These few targets show unexplained lines, but either do not agree in velocity or are possibly contaminated by ISM. Any that only contained one line or highly questionable lines were discarded as non-absorbers. We provide a target by target explanation in the Appendix.

3.2. Comparison

There have been two previous surveys of intrinsic UV absorption in low- z AGN, Crenshaw et al. (1999) and the preliminary survey by Kriss (2002). Crenshaw et al. had 17 targets in their C IV survey of data from the *Faint Object Spectrograph (FOS)* and the *Goddard High Resolution Spectrograph (GHRS)*. In the paper they labeled each of the targets as absorbers or non-absorbers, and we agree on all but one target of the 17, I Zw 1. Kriss had 16 targets which he identified with *FUSE* spectra as intrinsic absorbers. We disagree on three of the targets, I Zw 1, Mrk 304 and Mrk 478.

I Zw 1 is a weak C IV absorber in the spectrum taken by *FOS*. In the *FUSE* observation, I Zw 1 is in a low flux state. Thus, the O VI absorption lines may be present, but we label this target as a non-absorber because the potential lines are much like the surrounding noise. There is a line at approximately 1800 km^{-1} , but we only see it clearly in the O VI blue member. The other two are contaminated by H_2 . Mrk 304 and Mrk 478 have both been categorized as absorbers by Kriss (2002), but in our observations we find that Mrk 304 is only a possible absorber, and does not fit our conservative criteria. Mrk 478 shows no lines that cannot be explained by ISM contamination. Mrk 304 shows a possible line at 1800 km s^{-1} but it can only be seen in the O VI red member and Ly β . Thus by our standards, this object is only a possible absorber, and we do not include it as a firm detection. While NGC 7469 is a well known intrinsic absorber, the signal-to-noise of NGC 7469 combined with heavy H_2 contamination lead to a problematic spectrum.

Another survey we tested against was Laor & Brandt (2002), which used mostly *HST* data. While they had a broad range of redshifts and object types, there were a 14 objects that appeared in both of the studies. Of these 12 objects we agreed on 9. One object appears in both studies, but the signal-to-noise in the *FUSE* spectrum is too low for our study. Once again I Zw 1 and Mrk 304 are not absorbers on our list, but Laor & Brandt has classified them as absorbers. Mrk290 however is listed by Laor et al. as a non-absorber, while we see a distinct absorbing feature at approximately 200 km^{-1} .

4. Conclusions

For our final count we find of the 72 AGN with reasonably good signal-to-noise that 35 are intrinsically absorbing, with 11 new detections. Crenshaw et al. (1999) found approximately 60% of their sample show intrinsic absorption. In our survey, we find that 49% are absorbers. This could very well be a lower bound on the value due to the number of observations where the exposure times were not long enough to obtain a good signal-to-noise

for the object. So the sample may be slightly biased toward detecting absorption in AGN that are brighter in the far-UV.

An important quantity to be determined is the global covering factor (C_g), which is the fraction of the sky covered by the ensemble of absorbers as seen from the nucleus. This quantity is useful in helping us understand the geometry of the nucleus and the absorbing region. $C_g = F\langle C_f \rangle$, where F is the fraction of galaxies that show intrinsic absorption and $\langle C_f \rangle$ is the covering factor in the line of sight for the deepest component, averaged over all AGN with absorption. To estimate C_f for each individual AGN, we measured the residual flux (F_r) in the core of the deepest line. Assuming the component is saturated, and the residual flux is therefore unabsorbed continuum plus BLR flux (F_c), then $C_f = (1 - F_r/F_c)$. If the core is not saturated, which is unlikely in most cases, the value of C_f that we derived is actually a lower limit. Crenshaw et al. 1999 found $\langle C_f \rangle \approx 0.85$. We measured the residual flux in saturated lines in the *FUSE* data and found that $\langle C_f \rangle \approx 0.86$, very similar in both UV and far UV. So using $\langle C_f \rangle \approx 0.86$ with $F \approx 0.49$ we find a global covering factor of $C_g = 0.42$.

This measurement has also been made for other AGN samples. Ganguly et al. (2001) found a fraction of only 0.25 for C IV absorption in quasars with a $z < 1.0$, while the Laor & Brandt study found $F = 0.50$ for Seyferts and quasars up to redshifts of 0.5. George et al. (2000) found $F = 0.3$ for X-ray absorption in low- z quasars, and Vestergaard (2003) found $F = 0.55$ for quasars between 1.5 and 3.5 in redshift for C IV absorption. So for several luminosities and a wide range of redshift, most surveys find values for F around 1/2.

In our next paper, we will provide measurements by fitting these lines to find velocity centroids and equivalent width measurements. Once we have these values, we will examine each individual spectrum for variability in equivalent width, velocity and/or new components, which could lead to transverse velocities for the absorbers as seen in Kraemer et al. (2001).

This research has made use of the NASA/IPAC Extragalactic Database (NED) which is operated by the Jet Propulsion Laboratory, California Institute of Technology, under contract with the National Aeronautics and Space Administration. This research has also made use of NASA's Astrophysics Data System Abstract Service. We acknowledge support of this research under NASA grants NNG05GC55G, NNG06G185G and NAG5-13109.

We also would like to thank Dr. Charles Danforth for his technological expertise, advice and programming.

A. Notes on Individual Objects with Intrinsic Absorption

A.1. QSO 0045+3926

QSO 0045+3926 is a new intrinsic absorption discovery. We find that this object shows clear single line absorption in all three lines. The O VI region is found in the SiC portion of the spectrum; while the signal is lessened, there are no ISM lines nor any H₂ contamination.

A.2. Ton S180

Ton S180 shows very weak absorption, with some contamination from H₂ and a N II ISM line in the Lyman β line and no sign of H₂ absorption in the O VI red member. The Fe II ISM appears to be negligible based on the essentially non-visible nearby lines. This object was first seen as an absorber in Kriss (2002) but no intrinsic absorption was detected longward of 1200 Å.

A.3. Mrk 1044

Fields et al. (2005) have identified the same lines we found in the *FUSE* observation. The obvious component appears in both the O VI lines, but the Lyman β line is seriously contaminated via H₂. There is also evidence for a weaker line that appears to be slightly blended with Ar I in the O VI blue member, but is not clearly visible in O VI red and non-existent in Lyman β .

A.4. NGC 985

Absorption for this target was seen by Kriss (2002). Kriss lists this target with only one component, while we find that there are three narrow line absorbers with one blended broad absorber, which may consist of be two sub-components. The H₂ spectrum is varied in each of the O VI and Lyman β lines allowing for clear identification of each of these lines.

A.5. EUVE J0349-537

EUVE J0349-537 was first found in the EUVE survey and the optical counterpart was found by Craig and Fruschione (1997). Since that time it has appeared in 4 more surveys,

but no exorbitant amount of study has been placed upon it. This target shows one absorber that is broad enough that it is clearly above the noise, with a second nearby absorption feature that could be noise as it is only slightly visible in the O VI lines. This is a new absorption detection.

A.6. IRASF 04250-5718

This object originated in the Einstein Slew Survey (Elvis et al. 1992). We find at least two components absorbing in the far ultraviolet. It shows a broad component blended with a narrower component at a slightly lower velocity with very little contamination. This absorption has been seen previously by Kraemer et al. (1999).

A.7. Mrk 79

We see one component that is broad and shows very little contamination in the O VI lines. The Lyman β line is significantly weaker but still visible with little contamination. The second component is a narrow feature that is visible in the O VI red member, while the blue is highly contaminated and the $L\beta$ absorption is weak at best. This absorption has been identified previously. (Kraemer et al. 1999)

A.8. Mrk 10

This object shows H_2 interference in both of the O VI doublet lines, and Ar I ($\lambda 1067$) in the O VI red member. The absorption features are much too broad for H_2 and ISM absorption to completely explain them. Thus we find one or possibly two broad blending components. Mrk 10 has not been identified before as an intrinsically absorbing object.

A.9. IR 07546+3928

This object was found in the New Bologna Sky Survey (Ficarra et al. 1985); it has been flagged for possible C IV absorption studies with the *International Ultraviolet Explorer (IUE)* (Lanzetta et al. 1993). It has however not been labeled as an intrinsic absorbing target until now. In the *FUSE* observations there are two broad components which are heavily contaminated in the O VI blue member by Fe II ISM lines. The Ly β and the O VI

red member are fairly devoid of contamination.

A.10. PG 0804+761

While the spectrum of this object shows dayglow N I, the intrinsic absorption lines are evident with no clear interference from ISM. This object is a newly found intrinsic absorber.

A.11. Ton 951

Ton 951 was identified by Kriss in his 2002 conference paper. We find a single narrow absorption feature. Only one of the three available lines has any H₂ contamination.

A.12. IRAS 09149-62

One of the less well-studied AGN targets, IRAS 09149-62 shows broad absorption features across both members of the O VI doublet. The N II dayglow lines leave whether or not Ly β shows absorption to speculation. This detection is a first for this object.

A.13. Mrk 141

This spectrum is highly noisy and the continuum flux level is extremely low. There are two lines that are in the same place in velocity space from O VI, but this object is not an ideal example of an intrinsic absorber due to the lack of a Ly β line at that velocity. It was classified as an intrinsic absorber by Kriss (2002).

A.14. NGC 3516

We present in this paper 2 new observations of NGC 3516 taken by *FUSE*. There have been a total of 6 observations taken with *FUSE*. In the first observation Kriss (2002) identified the same components seen in FOS, STIS and GHRS data by Crenshaw et al. (1999) and Kraemer et al. (2001). Kraemer et al. showed that NGC 3516 shows variability in the absorption features, allowing them to find a lower limit on the transverse velocity of ~ 1800 km s⁻¹.

A.15. ESO 265-G23

This spectrum is full of H₂ features; however there is at least one absorption feature and two more possible components. The Ly β for the second possible component has a strong N II ISM line in it while the O VI red member is aligned with a Fe II ISM line. This is a new intrinsic UV absorption discovery.

A.16. NGC 3783

NGC 3783 was heavily studied by Gabel et al. (2005) using STIS and *FUSE* spectra. We find two broad components covering the span between -500 and -800 km s⁻¹, which agrees with Gabel et al. (2005). However Gabel et al. found a component at -1350 km s⁻¹ which is coincident with a feature in Ly β ; the O VI lines are somewhat less convincing in the *FUSE* spectrum.

A.17. NGC 4051

NGC 4051 shows a broad absorbing region that has no real contamination in the O VI blue member. The O VI red member is visible, but an O I dayglow line lies inside the trough and the Ly β has a similar problem with an O I dayglow line alongside the Ly β dayglow line. Using STIS, Collinge et al. (2001) found two absorbing systems, one at \sim -600 km s⁻¹ and one at \sim -2400 km s⁻¹. Each of these broad components break into up to 8 smaller components in STIS spectra in the C IV and N V lines. In the *FUSE* data we see only the lower velocity component. There is no evidence in the *FUSE* spectrum for a higher velocity component.

A.18. NGC 4151

Kraemer et al. (2006, and references therein) performed an in depth study on NGC 4151, which showed multiple components in STIS spectra. In the *FUSE* data we find multiple components blended together due to the sensitivity O VI to intrinsic absorption. The Ly β region is spoiled by the Ly β dayglow. We only provide the centroid of the velocity in Table 2 for this object.

A.19. RXJ 1230.8+0115

Due to the high redshift of RXJ 1230.8+0115, there is little interference from the ISM (only 3 Fe II lines). There appears to be at least one broad component with 2 other unexplained lines (1051 Å and 1050 Å) with two other broad absorption regions which do not have corresponding matches in velocity space. This was recognized by Ganguly et al. (2001) and attributed to intervening gas in the IGM.

A.20. TOL 1238-364

This object has been classified as a Seyfert 2 galaxy (NED), but there does seem to be evidence for a broad line region in the *FUSE* spectrum. We find 1 broad component that shows some contamination from H₂, Ar I, and C I. Because this has been labeled as a Seyfert 2 galaxy, it seems this object has not been considered as a target for intrinsic absorption studies.

A.21. PG 1351+640

PG 1351+640 has ample ISM contamination, but the overall absorption features look to be the same in all three lines. This was seen by Kriss (2002) and fitted by Zheng et al. (2001).

A.22. Mrk 279

Seen by Kriss (2002) and followed up with further study and Chandra observations by Scott et al. (2004), we find that there are three possible components. Of the three only one is free from question of contamination. The other two could be combinations of H₂ or ISM lines, however there seems to be a paucity of H₂ absorption in nearby regions of the spectrum. Two of the three features appear to be intrinsic absorption.

A.23. RXJ 135515+561244

This spectrum is in a very low continuum flux state, but shows evidence for one component of absorption with no contamination. This is a new intrinsic UV absorption discovery.

A.24. PG 1404+226

While the spectrum shows heavy ISM contamination, there are three absorption components uncorrupted in the O VI red member. These components agree in velocity with their O VI blue member and Ly β counterparts and have very little overlap with the ISM lines. This was a common target with the Laor & Brandt (2002) survey.

A.25. PG 1411+442

Laor & Brandt (2002) found that PG 1411+442 showed a large range of velocity for the intrinsic absorption (~ 5000 km/s). Unfortunately with the redshift for this object, the O VI region falls into the SiC portion of the spectrograph and provides less signal. We do not have enough signal to see the broad absorption Laor & Brandt found, but we have found two narrow components that are quite clear.

A.26. NGC 5548

NGC 5548 was found to be intrinsically absorbing by Shull & Sachs (1993) in data from *IUE* along with evidence of X-Ray warm absorption (George et al. 1998). Crenshaw et al. (1999) found absorption in FOS data as well. More recently Crenshaw et al. (2003) saw five blended and broad components in data from STIS. We see a similar case as Crenshaw et al. did in the FUSE data with five blended and broad components.

Brotherton et al. (2002) examined the *FUSE* data available prior to 2002 and found intrinsic absorption spanning the range between 0 and -1300 km s $^{-1}$, with is coincident with what we have found in our coadded spectrum.

A.27. Mrk 817

We consider this a weak absorber. Mrk 817 shows a weak absorption line that is isolated in the O VI blue member, and has a weak Fe II contaminate in the O VI red member. The Ly β is hardly visible, but this is easily understood due to the lower sensitivity of Ly β . This object has the fastest radial velocity component in a Seyfert galaxy to date (Table 2), as seen in Kriss (2002).

A.28. Mrk 290

Seen by Kriss (2002), the absorber is a narrow (~ 200 km/s FWHM) absorption component. There is some possibility for contamination in each of the three lines, however the amount of contamination can be estimated by nearby ISM features. Because the nearby features have larger oscillator strengths and are weak lines, this contamination must be small in our absorption features.

A.29. Mrk 876

Due to its higher redshift (0.129), the O VI doublet falls in the SiC region of the *FUSE* detector. But we still see a O VI broad line, with a few narrow absorption features that are most likely intrinsic, and have not been seen before.

A.30. Mrk 509

Mrk 509 shows absorption broad enough that it was first seen in data from *IUE* by York et al. (1984). It also shows evidence for an X-Ray warm absorber, as discussed in Reynolds (1997) and George et al. (1998). Kriss (2002) published the *FUSE* spectrum and identified the absorption components.

Kraemer et al. (2003) examined STIS data and found 8 components spanning the velocity range between -422 and $+210$ km s $^{-1}$. They performed photoionization models of the absorbers and found that they are not the same absorbing regions as the X-Ray absorbers.

In the *FUSE* observations with high resolution, in the Ly β absorption feature we see the two same broad absorbers, but due to the fact that the Ly β line is less sensitive, we can see that the two broad components are between 4 and 5 components, the fifth overlapping with a coincident H $_2$ line.

A.31. II Zw 136

Crenshaw et al. (1999) found two components in the FOS spectra for II Zw 136, which we see repeated in our *FUSE* observations. Component 1 is clearly visible and virtually free of ISM interference; component 2 however in the *FUSE* observations is clearly seen

only in the O VI red member. Ly β is weak at best and the O VI blue member is heavily contaminated with an Fe II line and two H₂ lines in the vicinity.

A.32. Akn 564

Akn 564 shows 2 broad and blended absorption components. H₂ lines heavily populate the area, but are far too narrow to account for the absorption. Crenshaw et al. (1999) saw absorption in the FOS data at the same central velocities we find. Romano et al. (2002) published the *FUSE* spectrum for this target and also identified the same components we find. Crenshaw & Kraemer (2001) found that this was 1 of 2 Seyfert galaxies that showed traits they characterized as a dusty lukewarm absorber.

A.33. IRASF 22456-5125

This object was seen first in the ROSAT wide field survey and later observed in the EUV. X-Ray studies have found this target to be highly variable (Grupe et al. 2001), but no ultraviolet intrinsic absorption has been previously identified. In our spectra we find 5 ‘finger-like’ narrow absorption components with little to no contamination from the ISM.

A.34. MR 2251-178

Ganguly et al. (2001), using FOS and STIS observations, found variability in the absorption in both velocity and column density. They found that the velocity of the component was ~ -1300 km s⁻¹, in data from STIS and FOS. We find that this object shows clear absorption in both Ly β and the O VI red member. While the blue member has both H₂ and ISM contamination, the velocity overlap is adequate enough to say that a significant portion of the absorption feature is intrinsic to the object.

The question for MR 2251-178 is whether the absorption is best aligned at -2000 km s⁻¹ where the Ly β absorption is weak and possible just ISM contamination, or at -300 km s⁻¹ where the O VI red member is weak. This could be a case of coincidental alignment where there are absorbers at both of these velocities; thus two of the features will be broader than the third component. Because X-Ray studies have shown this to be highly variable in X-Ray absorption (Halpern (1984)), and shown to be variable in the UV (Ganguly et al. 2001) it seems likely that the velocity on the component has shifted either accelerating to -2000 km s⁻¹ or decelerating to -300 km s⁻¹.

A.35. NGC 7469

NGC 7469 is a highly studied Seyfert 1 galaxy. Many surveys and studies to date have classified this as an intrinsically absorbing Seyfert galaxy (Scott et al. (2005), Kriss (2002), Crenshaw et al. (1999)). Thus this object is a known intrinsic absorber. In the *FUSE* data however, the absorption appears very weakly and in the Lyman β line there is a C II ISM line along with two heavy H₂ lines leaving doubt to the absorption feature. The O VI blue line is found at the same wavelength as Ar I (λ 1048 Å) which tends to be a strong ISM line in the far UV.

REFERENCES

- Anderson, K. S., & Kraft, R. P. 1969, *ApJ*, 158, 859
- Brotherton, M. S., Green, R. F., Kriss, G. A., Oegerle, W., Kaiser, M. E., Zheng, W. & Hutchings, J. B. 2002, *ApJ*, 565, 800
- Collinge, M. J. et al. 2001, *ApJ*, 557, 2
- Craig, N. & Fruscione, A. 1997, *ApJ*, 114.1356
- Crenshaw, D. M., Kraemer, S. B., Boggess, A., Maran, S. P., Mushotzky, R. F., & Wu, C.-C. 1999, *ApJ*, 516, 750
- Crenshaw, D. M., Kraemer & S. B. 2001, *ApJ*, 562L, 29
- Crenshaw, D. M., Kraemer, S.B., & George, I.M. 2003, *ARA&A*, 41, 117.
- Crenshaw, D. M., Kraemer & S. B. 2006, *astro.ph* 12446
- Cromwell, R., & Weymann, R. 1970, *ApJ*, 159, L147
- Dixon, W. V. D., Kruk, J. & Murphy, E. 2002, *The CalFUSE Pipeline Reference Guide*
- Dunn, J. P., Jackson, B., Deo, R. P., Farrington, C., Das, V., & Crenshaw, D. M. 2006, *PASP*, 118, 572
- Elvis, M., Plummer, D., Schachter, J., & Fabbiano, G. 1992, *ApJS*, 80, 257
- Feldman, P. D., Sahnou, D. J., Kruk, J. W., Murphy, E. M. & Moos, H. W. 2001, *JGR*, 106.8119
- Ficarra, A., Gruel, G., Tomassetti, G. 1985 *A&AS*, 59, 255
- Fields, Dale L., Mathur, S., Pogge, R. W., Nicastro, F., Komossa, S. & Krongold, Y. 2005, *ApJ*, 634, 928
- Gabel, J. et al. 2005, *ApJ*, 631, 741
- Ganguly, R., Charlton, J. C. & Eracleous, M. 2001, *ApJ*, 556L, 7
- George, I. M., Mushotzky, R. F., Turner, T. J., Yaqoob, T., Ptak, A., et al. 1998a, *ApJ*, 509, 146
- George, I. M., Turner, T. J., Yaqoob, T., Netzer, H., Laor, A., et al. 2000, *ApJ*, 531, 52
- Gillmon, K., Shull, J. M., Tumlinson, J. & Danforth, C. 2006, *ApJ*, 636, 891
- Grupe, D., Thomas H. C. & Beuermann, K. 2001, *A&A*, 367, 470
- Halpern, J. P. 1984, *ApJ*, 281, 90
- Lanzetta, K. M., Turnshek, D. A. & Sandoval, J. 1993, *ApJS*, 84, 109

- Kachikian & Weedman 1974, ApJ, 192, 581
- Kraemer, S. B., Turner, T. J., Crenshaw, D. M. & George, I. M. 1999, ApJ, 519, 69
- Kraemer, S. B., Crenshaw, D. M., & Gabel, J. R. 2001, ApJ, 557, 30
- Kraemer et al. 2003, ApJ, 582, 125
- Kraemer, S. B., Crenshaw, D. M., Gabel, J. R., Kriss, G. A., Netzer, H., Peterson, B. M., George, I. M., Gull, T. R., Hutchings, J. B., Mushotzky, R. F. & Turner, T. J. 2006, ApJS, 167, 161
- Kriss, G. A. 2002, ASPC, 255, 69
- Laor, A. & Brandt, W. N. 2002, ApJ, 569, 641
- Morton, D. C. 1991, ApJS, 77, 119
- Oke, J. B., & Sargent, W. L. W. 1968, ApJ, 151, 807
- Reynolds, C. S. 1997, MNRAS, 286, 513
- Romano, P., Mathur, S., Pogge, R. W., Peterson, B. M. & Kuraszkiewicz, J. 2002, ApJ, 578, 64
- Sahnou et al. 2000, ApJ, 538, 7
- Sahnou, D. 2002, The FUSE Instrument and Data Handbook
- Scott, J. E. et al. 2004, ApJS, 152, 1
- Scott, J. E. et al. 2005, ApJ, 634, 193
- Shull, J. M. & Sachs, E. R. 1993. ApJ, 416, 536
- Tumlinson, J. et al. 2002, ApJ, 566, 857
- Ulrich, M.-H., & Boisson, C. 1983, ApJ, 267, 515
- Vestergaard, M. 2003, ApJ, 599, 116
- York, D. G., Ratcliff, S. Blades, J. C., Wu, C. C., Cowie, L. L. & Morton, D. C. 1984, ApJ, 276, 92
- Zheng, W et al. 2001, ApJ, 562, 152Z

Fig. 1.— Plot of the spectrum of IRAS 04250-5718 in velocity space. The intrinsic absorption is visible in components between -300 and -50 km s^{-1} . The ISM tick marks are sized relative to oscillator strength, and the H_2 spectrum is the dashed curve. Between -1000 and -500 km s^{-1} there are possibly two ISM lines of Fe II that can be seen offset by approximately -50 km s^{-1} with respect to the observed frame. This gives us a good approximation for all Fe II lines across the spectrum.

Fig. 2.— We present all of the spectra for the targets we identified as intrinsic absorbers. The spectra are plotted in the observed frame and kinematic components of intrinsic absorption in the lines of $\text{Ly}\beta$ ($\lambda 1025.7$) and O VI ($\lambda\lambda 1031.9, 1037.6$) are numbered. Broad components are indicated by brackets. Strong narrow emission lines are geocoronal. The dashed line represents the synthetic H_2 spectrum. The specific velocity positions can be found in Table 2.

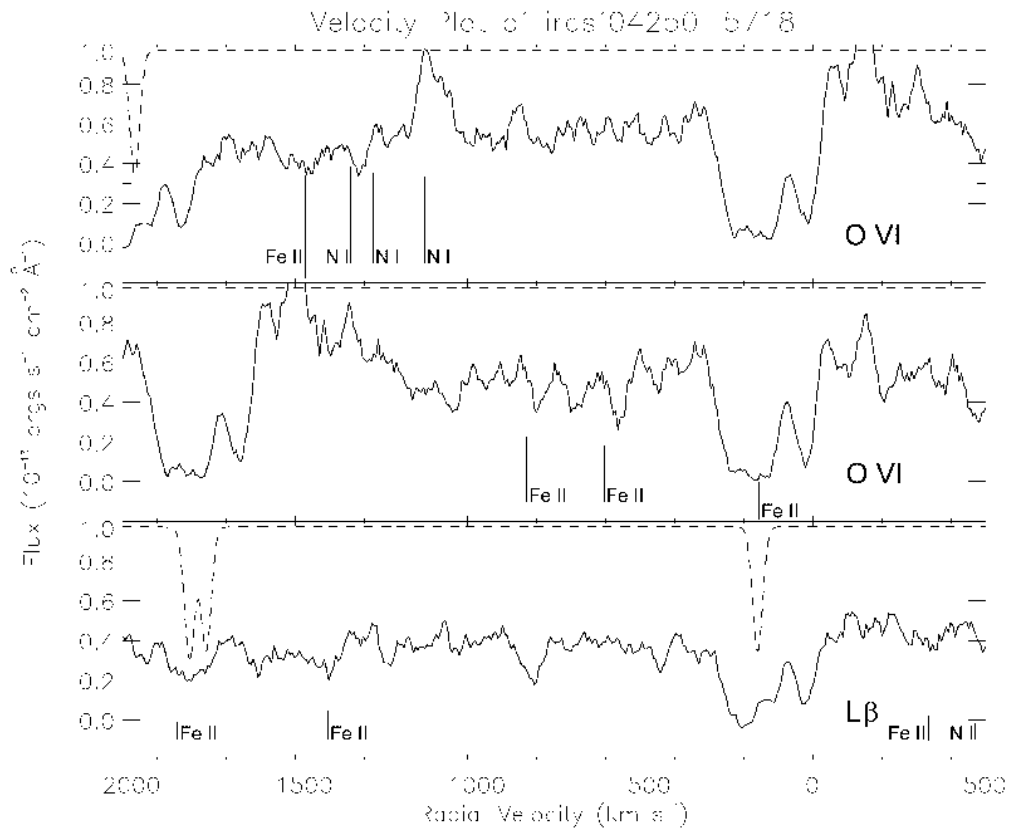


Fig. 1.

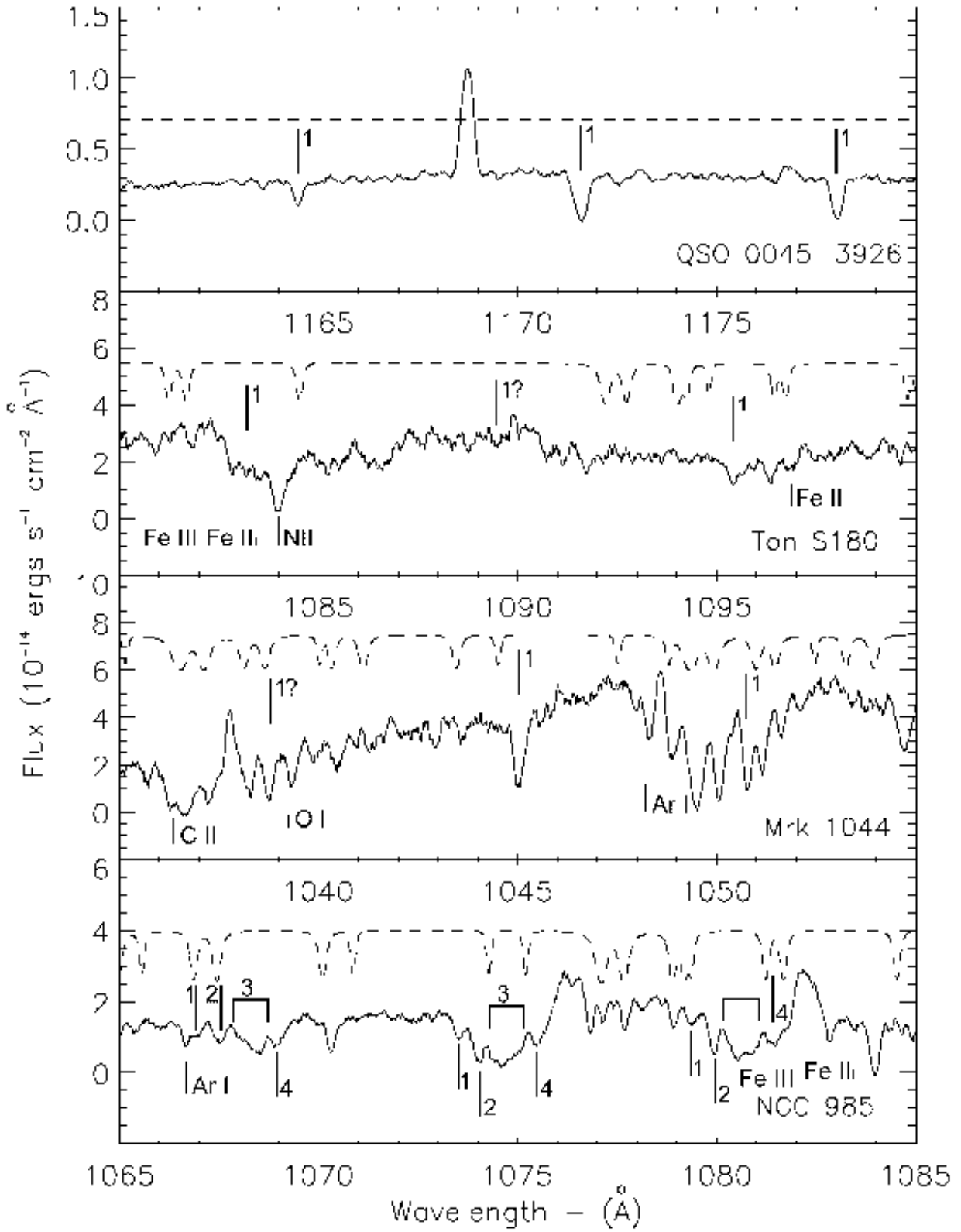


Fig. 2.

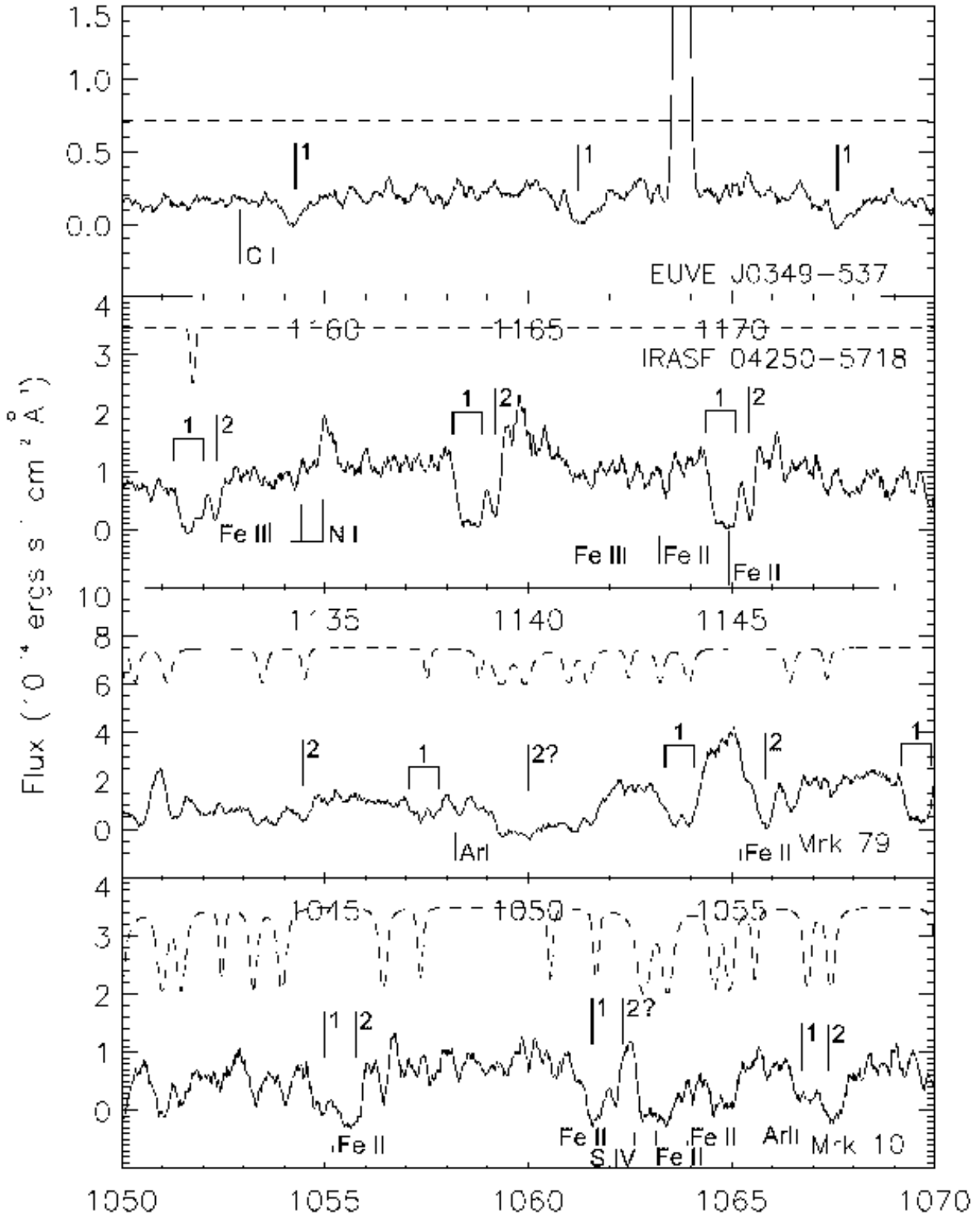


Fig. 2.

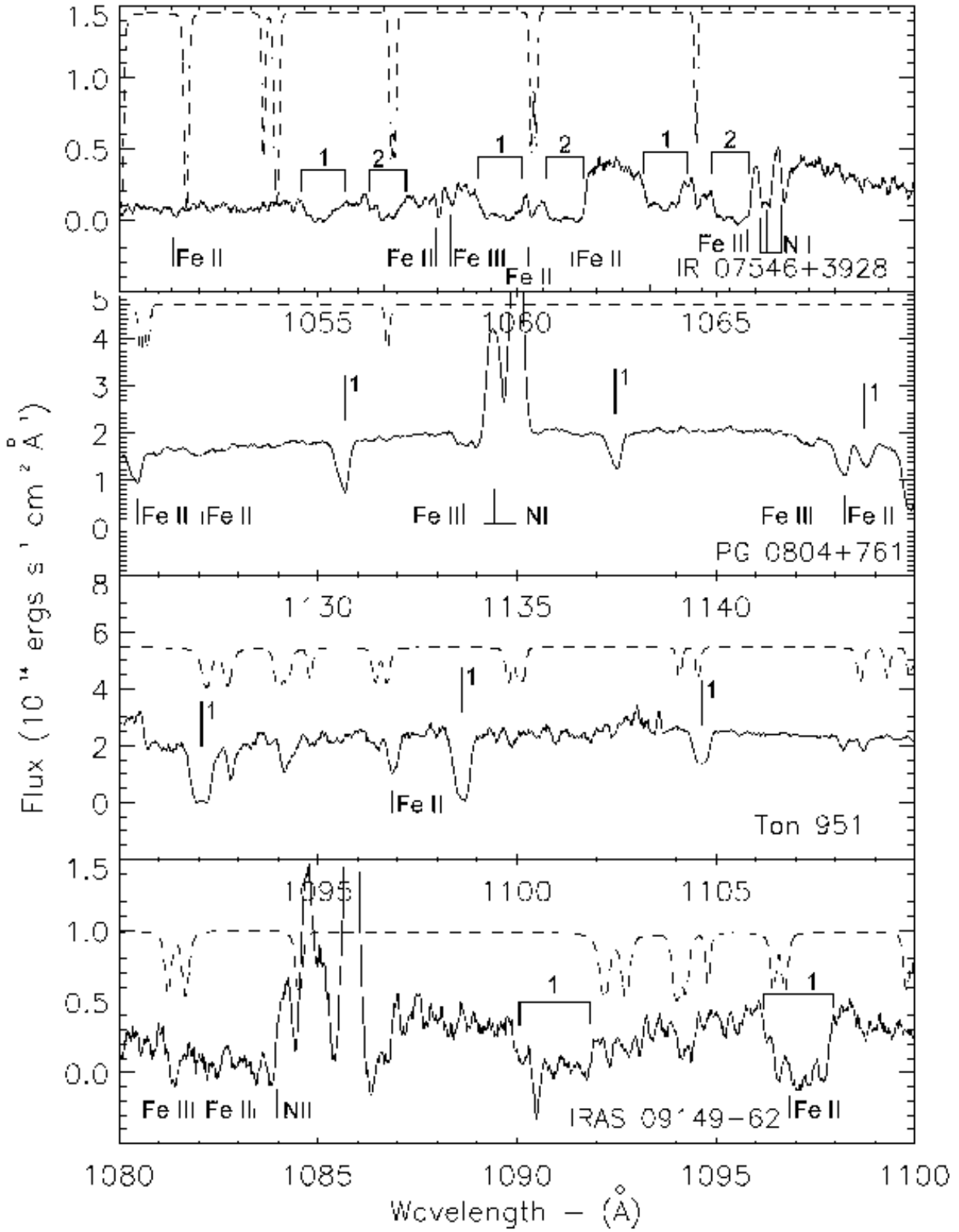


Fig. 2.

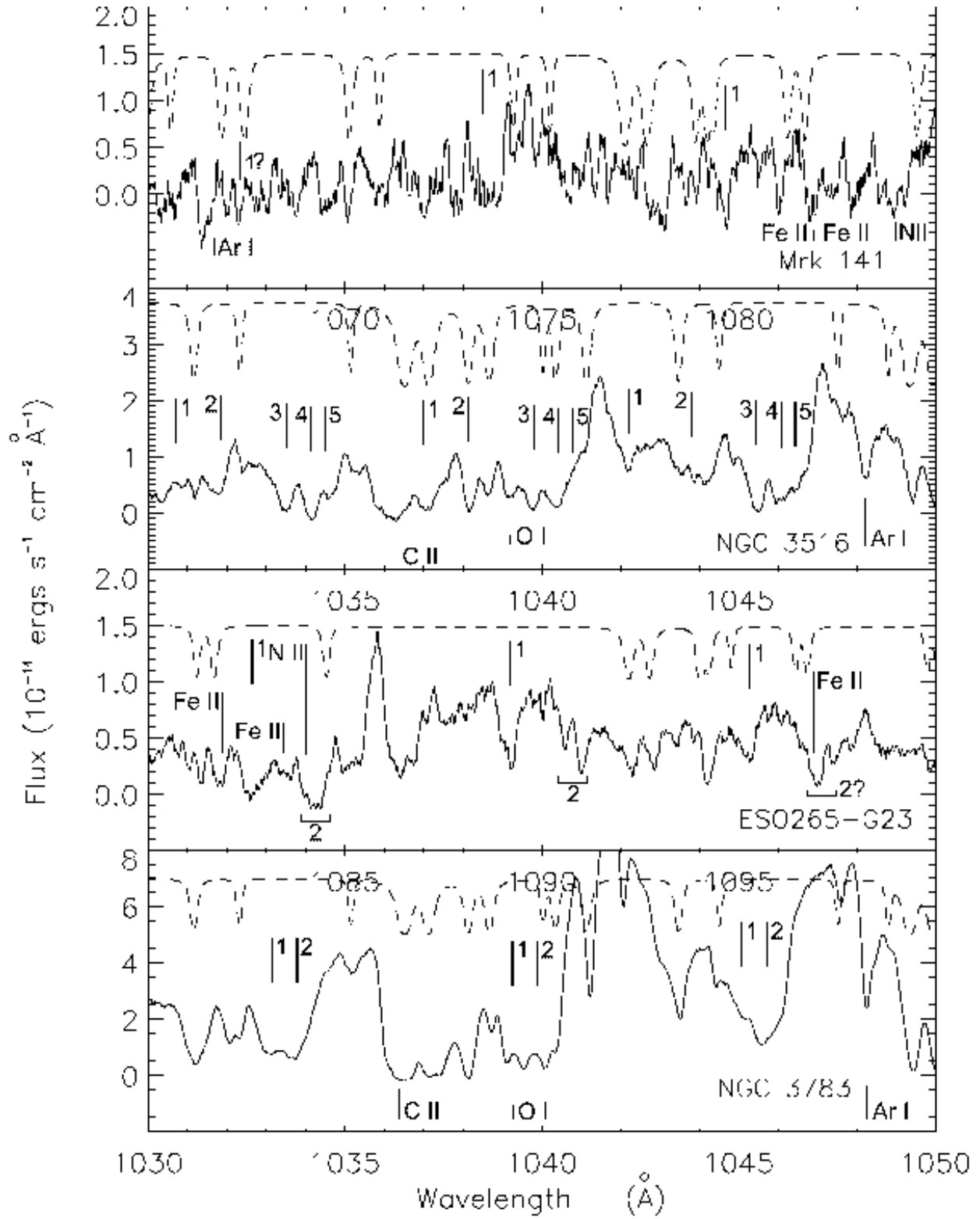


Fig. 2.

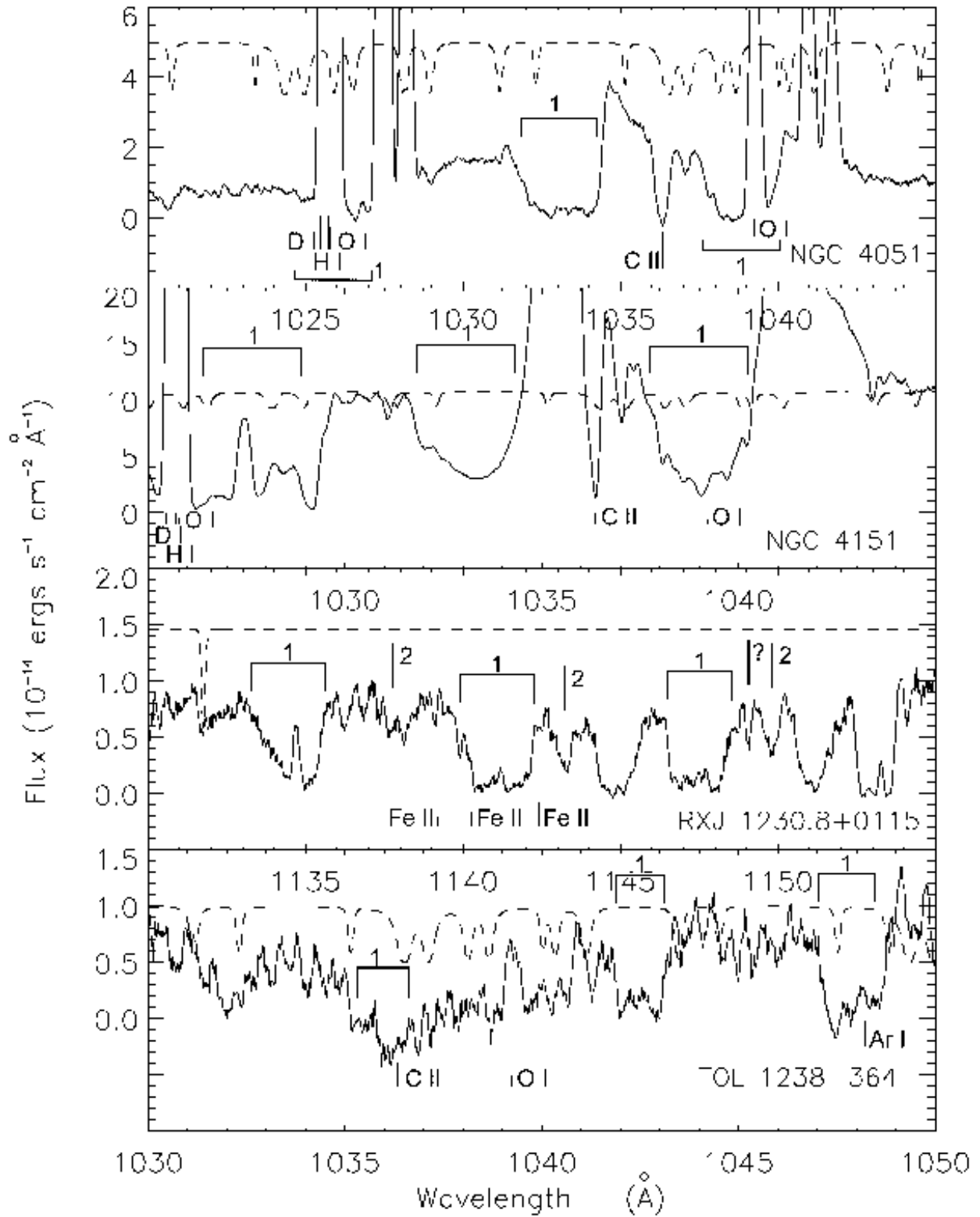


Fig. 2.

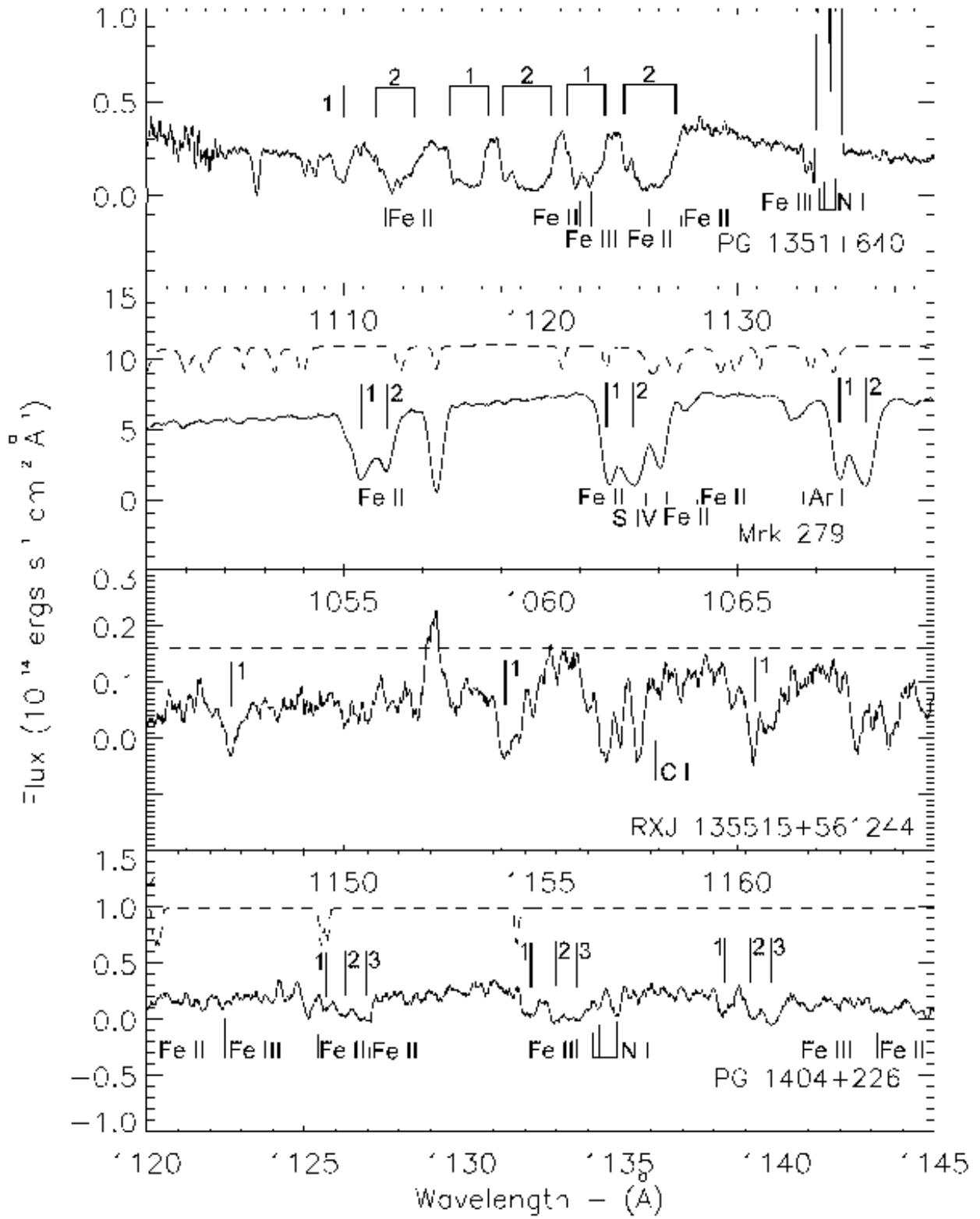


Fig. 2.

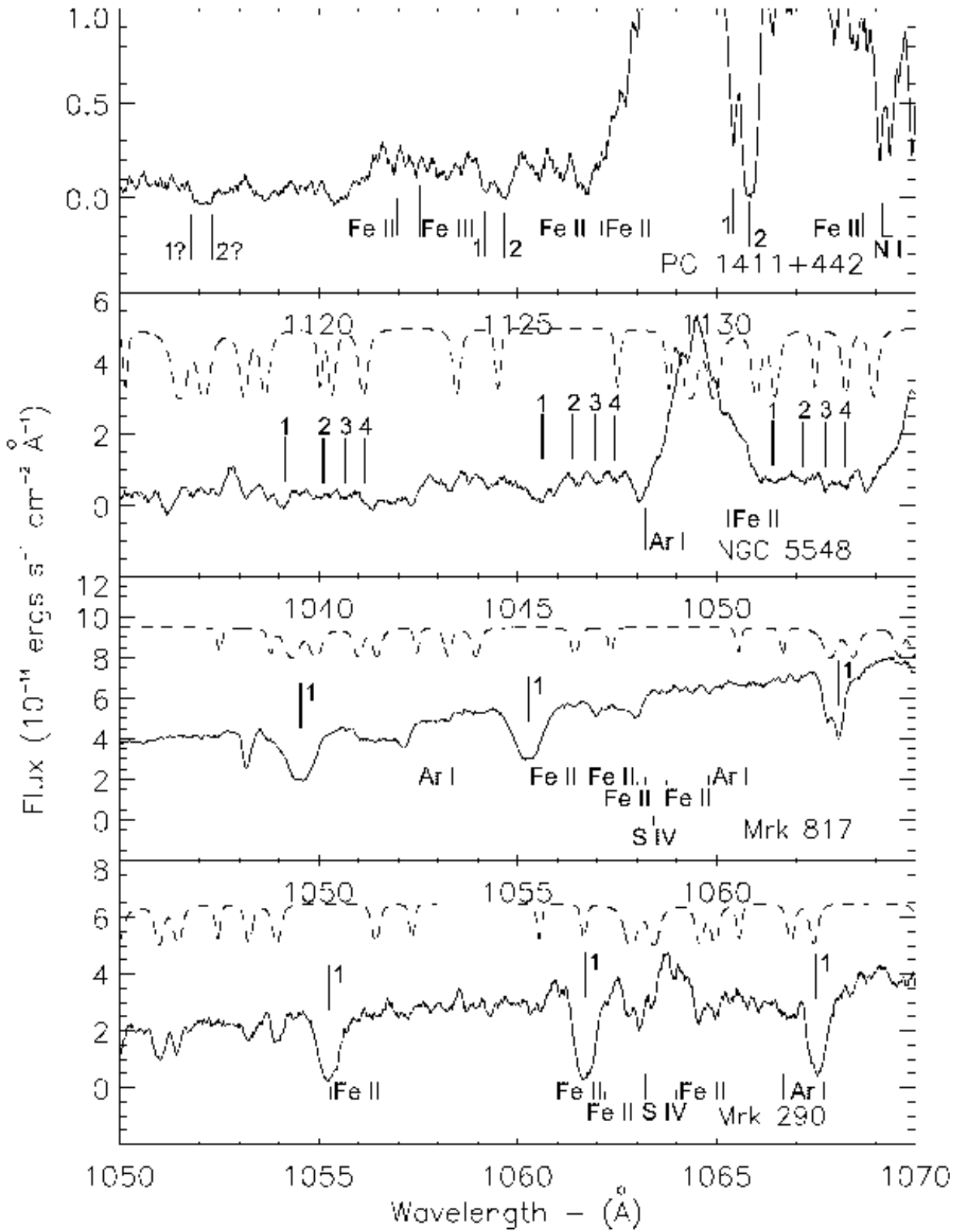


Fig. 2.

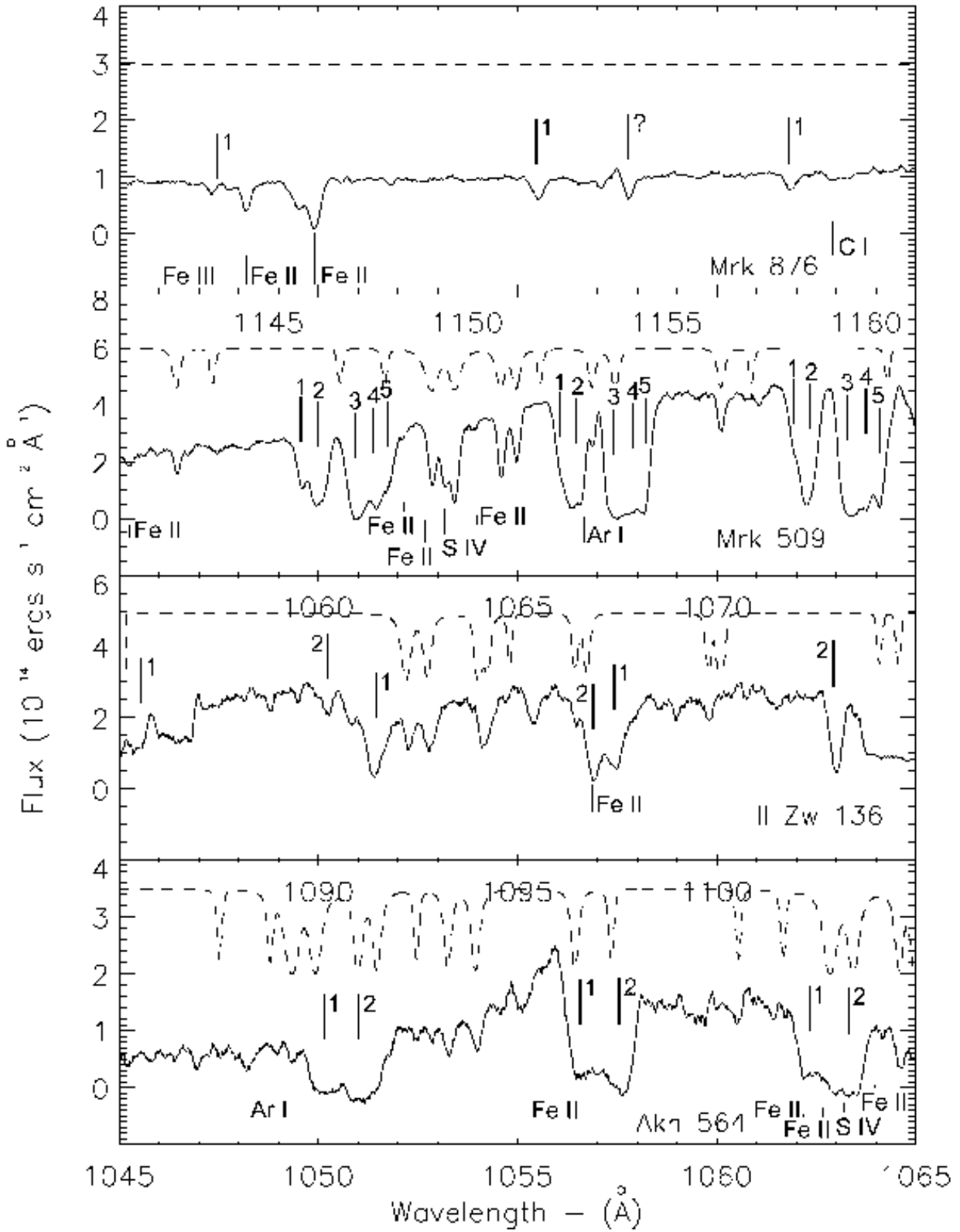


Fig. 2.

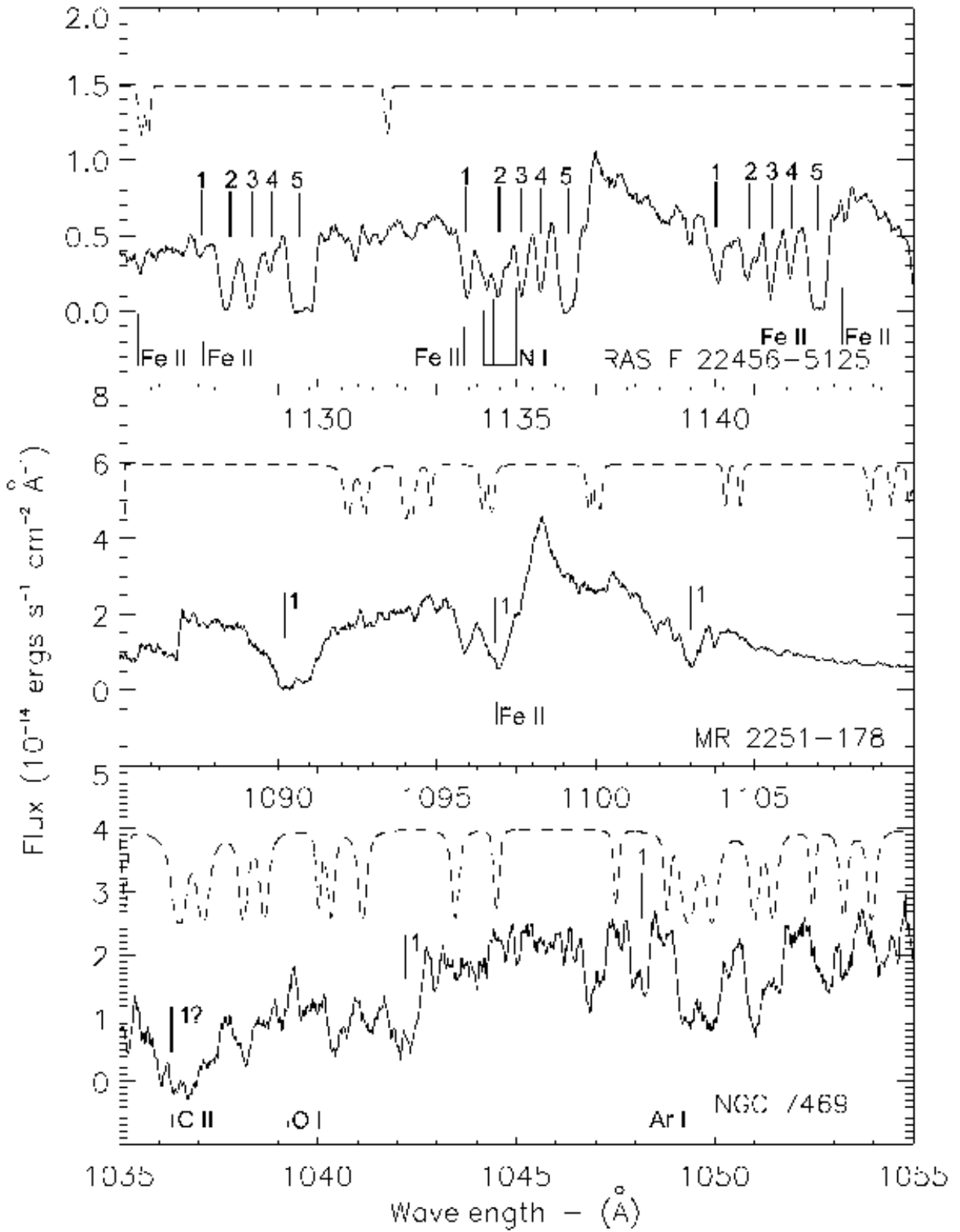


Fig. 2.

Table 1. AGN Included in the Survey

Object	RA	Dec	z	Class ^b	S/N	Observation ID	Observation Date	Exposure Time (s)
MRK335	00 06 19.53	+20 12 10.3	0.026	Sey 1.2	54.9	P1010204000	11/21/2000	53391
						P1010203000	12/4/1999	45894
QSO0045+3926	00 48 18.90	+39 41 12.0	0.134	Sey 1	9.6	D1310101000	10/8/2003	42658
						D1310105000	11/25/2004	25452
						D1310106000	11/26/2004	27487
						D1310104000	12/9/2003	40728
						D1310107000	11/27/2004	25058
						D1310102000	10/10/2003	34371
						Z0020401000	11/25/2000	8561
						D1310103000	10/11/2003	7272
I ZW 1	00 53 34.90	+12 41 36.0	0.061	Sey 1	3.8	P1110101000	12/3/1999	13584
						P1110102000	11/20/2000	25189
TONS180	00 57 19.95	-22 22 59.3	0.062	Sey 1.2	14.0	P1010502000	12/12/1999	15420
						D0280101000	7/13/2004	8955
MRK352	00 59 53.28	+31 49 36.7	0.015	Sey 1	3.7	P1070201000	10/11/1999	16644
RXJ010027-511346	01 00 27.06	-51 13 54.8	0.063	Sey 1	2.5	D8060301000	9/11/2003	6321
						E8970201000	8/22/2004	16845
TONS210	01 21 51.56	-28 20 57.3	0.116	Sey 1	23.0	P1070301000	10/21/1999	14023
						P1070302000	8/10/2001	41023
FAIRALL9	01 23 46.04	-58 48 23.8	0.047	Sey 1	12.54	P1010601000	7/3/2000	34896
MRK1044	02 30 5.45	-08 59 52.6	0.016	Sey 1	7.3	D0410101000	1/1/2004	12608
NGC985	02 34 37.77	-08 47 15.6	0.043	Sey 1	29.4	P1010903000	12/24/1999	49968
ESO31-8	03 07 35.30	-72 50 6.2	0.028	Sey 1	3.3	D9110201000	7/13/2003	15915
EUVEJ0349-537	03 49 28.50	-53 44 47.0	0.130	Sey 1	2.9	E8970301000	8/20/2004	27732
IRASF04250-5718	04 26 0.83	-57 12 0.4	0.104	Sey 1	2.1	D8080801000	9/4/2003	4895
FAIR303	04 30 40.02	-53 36 55.9	0.040	Sey 1	3.1	D8060702000	10/31/2003	16728
MRK618	04 36 22.25	-10 22 33.9	0.036	Sey 1	3.2	P1070901000	10/21/1999	2691
						P1070902000	12/7/2000	6293
AKN120	05 16 11.42	-00 08 59.4	0.033	Sey 1	12.2	P1011203000	12/31/2000	25617
						P1011201000	11/1/2000	8448
						P1011202000	11/3/2000	20942
PKS0558-504	05 59 47.40	-50 26 52.0	0.137	NL Sey 1	18.4	C1490601000	11/7/2002	48480
						P1011504000	12/10/1999	47271
IRASL06229-6434	06 23 9.10	-64 36 24.0	0.129	Sey 1	2.9	D9030304000	12/17/2003	14494
						U1071002000	7/19/2006	18569

Table 1—Continued

Object	RA	Dec	z	Class ^b	S/N	Observation ID	Observation Date	Exposure Time (s)
						D9030301000	12/14/2003	51104
						U1071001000	7/17/2006	11284
						D9030302000	12/16/2003	23363
						D9030303000	12/17/2003	11122
VIIZW118	07 07 13.10	+64 35 58.8	0.080	Sey 1	11.6	P1011606000	1/1/2000	9805
						P1011604000	10/6/1999	77568
						P1011605000	11/29/1999	26075
						P1011601000	10/2/1999	47515
						S6011301000	2/8/2002	47363
						P1011603000	10/2/1999	8957
1H0707-495	07 08 41.50	-49 33 5.8	0.041	Sey 1	12.8	B1050101000	11/16/2001	19989
						E1190101000	12/10/2004	50252
						B1050102000	3/6/2003	24260
						B1050103000	3/6/2003	22576
MRK9	07 36 57.02	+58 46 13.4	0.040	Sey 1.5	5.3	P1071102000	1/8/2000	14278
						P1071101000	11/29/1999	11829
						P1071103000	2/22/2000	10664
						S6011601000	2/11/2002	23555
MRK79	07 42 32.80	+49 48 34.9	0.022	Sey 1.2	3.0	P1011702000	1/14/2000	11688
						P1011701000	11/30/1999	3147
						P1011703000	2/22/2000	12498
MRK10	07 47 29.10	+60 56 1.0	0.029	Sey 1.2	2.7	Z9072801000	2/2/2003	22699
IR07546+3928	07 58 0.05	+39 20 29.1	0.096	Sey 1.5	6.7	P1071201000	3/9/2000	15290
						S6011801000	2/11/2002	27410
						E0870101000	11/7/2004	53151
PG0804+761	08 10 58.46	+76 02 41.9	0.100	Sey 1	28.3	S6011002000	2/9/2002	36886
						S6011001000	2/5/2002	58506
						P1011901000	10/5/1999	42715
						P1011903000	1/4/2000	21128
UGC4305	08 19 12.90	+70 43 6.0	0.001	Sey 1	11.1	F0270104000	12/20/2005	2210
						F0270102000	12/18/2005	28130
						F0270103000	12/19/2005	18821
PG0838+770	08 44 45.26	+76 53 10.0	0.132	Sey 1	2.62	G0200101000	2/10/2006	5942
						G0200104000	2/13/2006	35047
Ton951	08 47 42.60	+34 45 4.7	0.064	Sey 1	7.515	D0280304000	3/15/2004	10874

Table 1—Continued

Object	RA	Dec	z	Class ^b	S/N	Observation ID	Observation Date	Exposure Time (s)
						P1012002000	2/20/2000	30962
						D0280303000	3/15/2004 12:06	12774
						D0280302000	3/15/2004 3:50	12713
						D0280301000	3/14/2004 14:28	7935
IRAS09149-62	09 16 9.41	-62 19 29.5	0.057	Sey 1	6.45	S7011003000	3/31/2005	14520
						S7011002000	3/30/2005	13648
						A0020503000	2/6/2000	13157
						U1072201000	1/19/2006	7554
MRK110	09 25 12.87	+52 17 10.7	0.035	Sey 1	2.52	P1071302000	2/11/2001	10791
TON1187	10 13 3.21	+35 51 22.2	0.079	Sey 1	2.90	P1071502000	1/13/2000	7994
PG1011-040	10 14 20.58	-04 18 41.2	0.058	Sey 1	35.78	B0790101000	5/16/2001	85197
MKN141	10 19 12.59	+63 58 2.7	0.042	Sey 1.5	1.73	D8061001000	3/21/2004	15768
MKN142	10 25 31.28	+51 40 34.9	0.045	Sey 1	8.53	D8061101000	3/23/2003	20103
KUV-1031+398	10 34 38.61	+39 38 28.4	0.042	Sey 1	7.08	A0990101000	4/30/2000	53185
NGC3516	11 06 47.55	+72 34 6.9	0.009	Sey 1.5	1.91 ^a	P2110103000	1/28/2003	16753
						G9170101000	2/9/2006	28718
						P1110404000	4/17/2000	16335
						P2110102000	2/14/2002	20702
						P2110104000	3/29/2003	16125
						G9170102000	1/23/2007	16877
ESO265-G23	11 20 47.89	-43 15 50.6	0.056	Sey 1	3.2	A1210409000	4/29/2002	6428
						A1210405000	3/9/2001	4863
						A1210408000	4/28/2002	11487
						A1210407000	3/7/2002	21716
						A1210406000	2/28/2002	8381
						A1210404000	5/28/2000	1782
MRK734	11 21 47.11	+11 44 18.5	0.050	Sey 1.2	3.1	P1071702000	4/16/2001	4587
NGC3783	11 39 1.78	-37 44 18.5	0.010	Sey 1	21.6	B1070103000	3/11/2001	27221
						B1070104000	3/30/2001	25180
						B1070105000	6/27/2001	27483
						B1070106000	3/7/2001	25541
						P1013301000	2/2/2000	37003
						E0310101000	5/5/2004	23286
						B1070102000	2/28/2001	26645
IR1143-1810	11 45 40.48	-18 27 15.3	0.033	Sey 1	8.51	P1071901000	5/29/2000	7243

Table 1—Continued

Object	RA	Dec	z	Class ^b	S/N	Observation ID	Observation Date	Exposure Time (s)
NGC4051	12 03 9.61	+44 31 52.8	0.002	Sey 1.5	7.26	B0620201000	3/29/2002	28659
						C0190102000	3/19/2003	28594
						C0190101000	1/18/2003	13933
NGC4151	12 10 32.60	+39 24 21.0	0.003	Sey 1.5	61.79	P2110201000	4/8/2001	13612
						P2110202000	6/1/2002	5953
						C0920101000	5/28/2002	48892
						P1110505000	3/5/2000	21522
PG1211+143	12 14 17.61	+14 03 12.7	0.081	Sey 1	40.02	P1072001000	4/25/2000	52274
MRK205	12 21 44.04	+75 18 38.3	0.071	Sey 1	24.71	S6010801000	2/2/2002	16027
						D0540101000	11/13/2003	19618
						D0540103000	11/17/2003	19131
						Q1060203000	12/29/1999	37051
						D0540102000	11/14/2003	114015
NGC4395	12 25 48.92	+33 32 48.4	0.001	Sey 1	4.39	C0860101000	2/25/2003	36484
RXJ1230.8+0115	12 30 50.00	+01 15 22.7	0.117	Unk ^c	2.79	P1019001000	6/20/2000	4031
PG1229+204	12 32 3.62	+20 09 29.4	0.063	Sey 1	2.62	P1072301000	2/5/2001	6267
TOL1238-364	12 40 52.90	-36 45 21.1	0.011	Sey 2?	4.67	D0100101000	6/13/2003	17912
PG1351+640	13 53 15.80	+63 45 45.0	0.088	Sey 1	15.42	S6010701000	2/1/2002	48620
						P1072501000	1/18/2000	70134
MRK279	13 53 3.52	+69 18 29.7	0.030	Sey 1.5	53.24	P1080304000	1/11/2000	30747
						F3250103000	12/7/2005	2289
						C0900201000	5/18/2002	41708
						D1540101000	5/12/2003	91040
						F3250104000	12/8/2005	3187
						F3250106000	2/3/2006	3703
						P1080303000	12/28/1999	60338
RXJ135515+561244	13 55 16.55	+56 12 44.6	0.122	Sey 1	1.78	D8061601000	3/13/2003	47223
PG1404+226	14 06 22.15	+22 23 42.8	0.098	Sey 1	1.86	P2100401000	6/11/2001	11489
PG1411+442	14 13 48.32	+44 00 13.1	0.090	Sey 1	2.64	A0601010000	5/11/2000	7360
PG1415+451	14 17 0.84	+44 56 6.0	0.114	Sey 1	2.47	A0601111000	5/10/2000	12285
NGC5548	14 17 59.91	+25 08 12.6	0.017	Sey 1.5	11.11	D1550102000	2/11/2004	7757
						P1014601000	6/7/2000	25932
						D1550101000	2/10/2004	22229
MRK1383	14 29 6.60	+01 17 6.6	0.086	Sey 1	22.27	P1014801000	2/18/2000	25051
MRK817	14 36 22.09	+58 47 39.5	0.031	Sey 1.5	49.78	P1080404000	2/18/2001	86013

Table 1—Continued

Object	RA	Dec	z	Class ^b	S/N	Observation ID	Observation Date	Exposure Time (s)
						P1080402000	2/18/2000	12911
						P1080401000	2/17/2000	12119
						P1080403000	12/23/2000	71804
MRK477	14 40 38.06	+53 30 15.7	0.038	Sey 1	7.25	P1110808000	5/8/2001	11289
MRK478	14 42 7.46	+35 26 22.9	0.079	Sey 1	1.86	P1110909000	1/29/2001	14118
MRK290	15 35 52.38	+57 54 9.3	0.030	Sey 1	5.53	D0760101000	6/28/2003	9239
						D0760102000	2/27/2004	46032
						P1072901000	3/16/2000	12769
						E0840101000	6/15/2004	11931
MRK876	16 13 57.21	+65 43 9.7	0.129	Sey 1	37.02	P1073101000	10/16/1999	52659
						D0280201000	5/16/2003	11786
						D0280203000	2/14/2004	73334
PG1626+554	16 27 56.09	+55 22 32.0	0.133	Sey 1	2.15	P1073201000	2/18/2000	9754
						C0370101000	5/20/2002	91237
MRK506	17 22 39.92	+30 52 53.1	0.043	Sey 1	4.34	P1073401000	6/8/2000	10430
3C382	18 35 3.38	+32 41 47.0	0.058	Sey 1	3.15	P1073701000	6/9/2000	11297
PKS2005-489	20 09 25.39	-48 49 53.7	0.071	QSO	6.97	C1490301000	4/12/2002	24726
						C1490302000	6/4/2002	13422
MRK509	20 44 9.74	-10 43 24.7	0.034	Sey 1.2	42.83	P1080601000	9/5/2000	60656
						X0170102000	11/6/1999	33410
						X0170101000	11/2/1999	20004
IIZW136	21 32 27.83	+10 08 19.4	0.063	Sey 1	11.55	P1018301000	11/14/2000	22629
						P1018302000	5/27/2004	11497
						P1018303000	5/28/2004	8067
						P1018304000	11/1/2004	21872
MRK304	22 17 12.28	+14 14 20.9	0.066	RQQ	3.05	P1073901000	7/16/2000	12387
AKN564	22 42 39.34	+29 43 31.3	0.025	Sey 1.8	6.19	B0620101000	6/29/2001	55515
IRASF22456-5125	22 48 41.00	-51 09 54.0	0.100	Sey 1	6.82	Z9073902000	9/24/2002	31301
						Z9073901000	9/24/2002	5534
MR 2251-178	22 54 5.80	-17 34 55.0	0.064	Sey 1	16.13	P1111010000	6/20/2001	54113
NGC7469	23 03 15.62	+08 52 25.6	0.016	Sey 1.2	2.22	C0900101000	12/13/2002	3593
						C0900102000	12/14/2002	3352
						P1074101000	6/28/2000	13217

^aReduced from a possible S/N of 3.34.

^bAGN types listed in the NASA Extragalactic Database

^cNo AGN type listed

Table 2. Objects with Intrinsic Absorption in the Survey

Object	Component Velocities (km s ⁻¹)
QSO0045+3926	1) +340
TONS180	1) -1800
MRK1044	1) -1100, 2) -270
NGC985	1) -700, 2) -410, 3) -290
EUVEJ0349-537	1) 0
IRASF04250-5718	1) -200, 2) -100, 3) -20
MRK79	1) -1400, 2) -320
MRK10	1) -150, 2) -200
IR07546+3928	1) -1800, 2) -1200
PG0804+761	1) +700
TON951	1) +160
IRAS09149-62	1) 0
MKN141	1) -600
NGC3516	1), -1320 2), -830 3), -370 4), -180 5) -60
ESO265-G23	1) -150, 2) +400
NGC3783	1) -700
NGC4051	1) -300
NGC4151	1) -500
RXJ1230.8+0115	1) -3000, 2) -2000, 3) +400
TOL1238-364	1) -200
PG1351+640	1) -1800, 2) -1000
MRK279	1) -450, 2) -280
RXJ135515+561244	1) -990, 2) -780, 3) -220, 4) -110, 5) -0
PG1404+226	1) -290, 2) -20, 3) +150
PG1411+442	1) -50, 2) +80
NGC5548	1) -700, 2) -480
MRK817	1) -4100
MRK290	1) -220
MRK876	1) -3800
MRK509	1) -400, 2) -290, 3) -10, 4) +120, 5) +200
IIZW136	1) -1500, 2) +20
AKN564	1) -250, 2) 0
IRASF22456-5125	1) -350, 2) -150, 3) +100, 4) +150, 5) +350
MR 2251-178	1) -2000 or -300
NGC7469	1) -1900

